Impedance and Nonlinear Dielectric Testing at High AC Voltages Using Waveforms

Jan Obrzut, *Member, IEEE,* and Kenji Kano

Abstract—This paper presents the application of a waveform technique that can determine the complex impedance and nonlinear response of dielectric composite films at high ac voltages using a data acquisition (DAQ) card and virtual instrumentation. The voltage waveforms are Fourier transformed from the time domain to the frequency domain to obtain the fundamental and higher order harmonic responses as complex phasor quantities. The specimen impedance is determined by performing complex algebraic calculations. It was found that the conventional fiber-glass reinforced epoxy resin laminates exhibit a flat impedance characteristic, nearly independent of voltage, up to near breakdown conditions. At near breakdown conditions, the second-harmonic response starts to decrease, indicating a dielectric softening of the material. At higher voltages, nonlinear dielectric behavior is dominated by the third-harmonic response. In contrast, the impedance of dielectric hybrid materials made of organic resins and high-dielectric constant ceramics decreases continuously with increasing voltage. The drop in impedance is accompanied by a reversible transformation from a dielectric to resistive character. The field-induced nonlinear dielectric effects are mainly due to polarization reversal of the high-k filler, which is manifested by a large third-harmonic response. The near breakdown conditions in such materials can be inferred from the second-harmonic response, which diminishes when the ac electric field erases the residual static polarization. The presented testing procedure represents a compatible extension of the existing standard test methods for dielectric breakdown but is better suited for testing thin-film materials with a high-dielectric constant. The results demonstrate that the voltage withstanding condition can be inferred from the impedance characteristic and the nonlinear dielectric response without ambiguity.

Index Terms—AC harmonics, complex impedance, dielectric breakdown voltage, dielectric hybrid materials, nonlinear dielectric response, waveform measurements.

I. INTRODUCTION

THIN dielectric composite films with enhanced electrical and mechanical properties are used in electronics as building blocks of functional circuits and as the insulation materials for power distribution. The electrical performance of these materials can be evaluated by measuring the dissipation current, breakdown voltage, and/or dielectric loss tangent. The conventional standard testing procedures that are currently in use have been developed for thick high-impedance dielectrics [1] and measure performance in terms of breakdown voltage. Since the impedance of thin dielectric films and those with a high dielectric constant is rather low, conventional measurement procedures are inadequate and may lead to ambiguous results.

The conventional testing techniques use either dc or ac current [2]. However, ac testing voltage is preferred, especially for asymmetric metal-insulator configurations that may have rectifying characteristics and for high-k composite materials that exhibit dielectric saturation and/or polarization reversal. Under ac high field, the dielectric response can be nonlinear.

Monitoring and analysis of both the incident voltage and the resulting current waveforms is a more useful mean for proper evaluation of the dielectric responsiveness. Venkatesh and Naidu used a capacitance divider and a digital storage oscilloscope to capture waveforms [3]. Tanaka *et al.* developed a system that monitors the dissipation current waveforms for a capacitive load using a capacitance bridge and a digital oscilloscope [4], [5]. The measurement of nonlinear dielectricity in ferroelectric polymers using computerized DAQ and digital Fourier transform techniques was described by Furukawa *et al.* [6]. To date, no published successful attempt has been made to measure complex impedance, the phase component of the dissipation current as a function of a high ac voltage.

This paper describes a measurement technique for recording and analyzing the incident voltage and the resulting dissipation current waveforms at fundamental frequency and higher order harmonics using a multichannel DAQ card.[1] This technique is applied to determine the complex impedance and nonlinear dielectric response at high ac voltages. The effect of high voltage on the electrical performance of materials and nonlinear dielectric response is demonstrated for conventional glass-fiber epoxy resin laminates and for novel composites with enhanced dielectric properties.

II. EXPERIMENTAL SETUP

The availability of computerized DAQ systems makes it convenient to record a digitized spectrum of the entire voltage wave as a function of time. In contrast to the conventional procedures that utilize engineering notation, recording the voltage waves and transforming the data from the time domain to the frequency domain enables the determination of phase between the voltage and the current waves and, consequently, the complex impedance $\vec{Z}$. Fig. 1 shows the block diagram of the measurement system. An IEEE 488.2 bus is connected to a computer

---

[1]Certain equipment, instruments, or materials are identified in this paper in order to adequately specify the experimental details. Such identification does not imply recommendation by the National Institute of Standards and Technology nor does it imply the materials are necessarily the best available for the purpose.
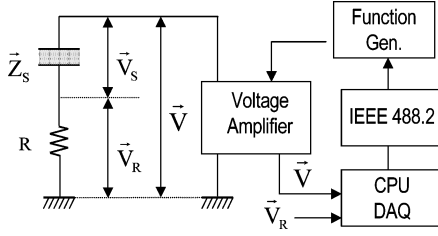
Fig. 1. Measurement diagram.

to control the instruments using standard command for programmable instruments language. An IEEE 488.2-controlled function generator (Agilent 33 250A) is used to source a sinusoidal voltage wave at a frequency f. The source voltage wave is amplified by an operational voltage amplifier (Trek Model 610C), and a high ac voltage is applied to the specimen. The specimen current is monitored using a standard reference resistor R as shown in Fig. 1. Separate channels of the DAQ card record the waveform of the monitoring signal (which is proportional by a gain factor to the output voltage $\vec{V}$ from the voltage amplifier), and the voltage wave at the reference resistor $\vec{V}_R$ (which is proportional to the specimen current). We used a two-channel 12-b analog–digital (A/D) converter (NI-6111) clocked at a frequency of 20 MHz, which has the capability of simultaneously sampling both channels at frequencies of up to 100 kHz. The sampling was assumed coherent, i.e., containing an integer number of the sine-wave periods and an integer number N of the data points. In our experiments, $N = 1000$ and $f = 50$ Hz ± 0.001 Hz. The discrete quantization time and amplitude errors [7], [9] were assumed to be within the manufacturer's specification for the NI-6111.

The experimental uncertainty depends primarily on the tolerance of the reference resistor and its phase characteristic. The combined relative uncertainty was 0.5% for the measured voltage wave amplitude and 1.5% for the phase.

III. ANALYSIS

In the time domain, the voltage and the current alternating at frequency f are periodic functions of time t that can be expressed as waveforms $v(t) = v_o \cos(\omega t + \varphi)$ and $i(t) = (v_{Io}/R) \sin(\omega t)$, where v_o is the voltage amplitude, (v_{Io}/R) is the current amplitude, $\omega = 2\pi f$, and φ is the phase angle between the voltage and the resulting current flowing through a reference resistor R. In engineering notation, the root-mean-square (rms) or effective voltage and current are defined as $V = v_o/\sqrt{2}$ and $I = (v_{Io}/R)/\sqrt{2}$, respectively. However, in the case of complex loads such as capacitance C or inductance L, there will be a phase shift φ between V and I. In general, the alternating voltage and the current can be expressed as phasor transforms from the time domain to the frequency domain representing complex quantities, each having an amplitude and phase. The quotient of the voltage phasor $\vec{V}$ and the current phasor $\vec{I}$ represents the complex circuit impedance $\vec{Z}$. A waveform digitized to N points, where $v(l)$ represents an individual voltage data point recorded at the

time $t_l = (2\pi l)/(\omega N)$, can be expressed as a sum of the phasor components V′ and V″:

$$v(l) = \text{V}' \cos\left(\frac{2\pi l}{N}\right) + \text{V}'' \sin\left(\frac{2\pi l}{N}\right). \tag{1}$$

Using the discrete Fourier transform technique (DFT) [6], [8], the wave can be transferred from the time domain to the frequency domain by calculating V′ and V″ from (2) and (3):

$$\text{V}' = \frac{2}{N} \sum_{l=1}^{N} \text{v}(l) \cos\left(-\frac{2\pi l}{N}\right) \tag{2}$$

$$\text{V}'' = \frac{2}{N} \sum_{l=1}^{N} \text{v}(l) \sin\left(-\frac{2\pi l}{N}\right) \tag{3}$$

where $2/N$ represents the normalization factor.

The phasor amplitude V_0 and its initial phase angle δ_0 in the frequency-domain representation of the waveform can be calculated from (4) and (5), respectively, as follows:

$$\text{V}_0 = \sqrt{(\text{V}')^2 + (\text{V}'')^2} \tag{4}$$

$$\delta_0 = \arctan\left(\frac{\text{V}''}{\text{V}'}\right). \tag{5}$$

The applied voltage $\vec{V}$ can be expressed in exponential notation by

$$\vec{V} = \text{V}_0 \exp(j(\omega t + \delta_0)) \tag{6}$$

where the initial phase δ_0 is given by (5).

Similarly, the voltage $\vec{V}_R$ can be determined using expressions (2)–(5) and represented in exponential notation

$$\vec{V}_R = \text{V}_{R0} \exp(j(\omega t + \varphi + \delta_0)) \tag{7}$$

$$\varphi + \delta_0 = \arctan\left(\frac{\text{V}_R''}{\text{V}_R'}\right) \tag{8}$$

where φ is a phase shift between $\vec{V}$ and $\vec{V}_R$. The complex impedance of the specimen $\vec{Z}_S$ can be obtained from

$$\vec{Z}_S = R\left(\frac{\vec{V}}{\vec{V}_R} - 1\right). \tag{9}$$

One can perform further analysis of the material's linear and nonlinear dielectric properties, such as the dielectric loss tangent and the higher order harmonic component of the current response wave as a function of the specimen voltage $\vec{V}_S = \vec{V} - \vec{V}_R$. The amplitude of the nth-order harmonic response i_n can be calculated from

$$i_n = \frac{2}{N}\left[\left\{\sum_{l=1}^{N} \frac{v_R}{R}(l) \cos\left(\frac{2\pi nl}{N}\right)\right\}^2 + \left\{\sum_{l=1}^{N} \frac{v_R}{R}(l) \sin\left(\frac{2\pi nl}{N}\right)\right\}^2\right]^{1/2} \tag{10}$$
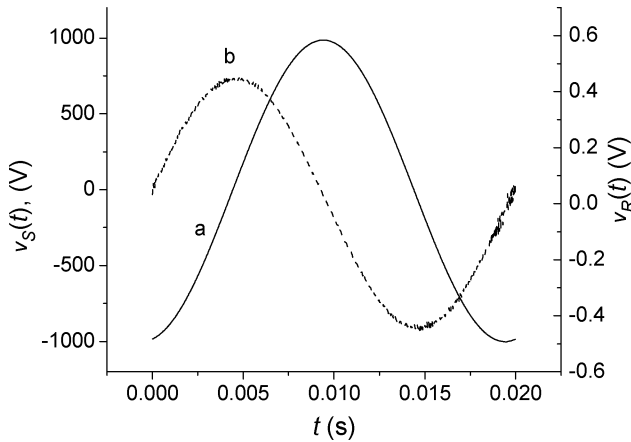
Fig. 2.   Voltage waveforms for FR-4 specimens: (a) $-v_S(t)$ and (b) $-v_R(t)$.

where $(v_R/R)(l)$ represents an individual data point of the specimen current, $i(l)$, recorded at the time $t_l = (2\pi l)/(\omega N)$ and n $(1, 2, 3, \ldots)$, is the harmonic order [9].

The DFT, and all the complex algebra calculations can readily be accomplished within a framework of integrated virtual instrumentation software.

IV.   RESULTS AND DISCUSSION

In order to verify the proposed procedure experimentally, we implemented the experimental setup shown in Fig. 1 and performed impedance measurements on several fiber-glass reinforced epoxy resin laminates and on newly developed hybrid materials with enhanced dielectric properties. Here, we present results obtained for a 50-μm-thick FR-4 epoxy resin laminate and for a 40-μm-thick dielectric composite made of an organic resin filled with ferroelectric ceramic submicrometer-size particles. Both materials are representative of high-capacitance layers that are being used in advanced electronic circuits for power–ground decoupling. The test pattern was made in accordance to the American Society for Testing and Materials (ASTM) standard [1], with a diameter of the top electrode of 14.1 mm. Fig. 2 shows an example of typical waveforms obtained for the FR-4 samples at 50 Hz. The response waveform $v_R(t)$ is a corresponding sinusoid of the specimen voltage $v_S(t)$. Since the time lag τ_0 between $v_S(t)$ and $v_R(t)$ is about -5 ms, the phase shift ($\varphi = 2\pi f\tau_0$) is about $-90°$, indicating that the FR-4 sample has a capacitive character. The impedance and phase plots as a function of the specimen voltage are shown in Fig. 3. The impedance magnitude remains at a level of about 22.3 MΩ up to 1.7 kV. Above 1.7 kV, the impedance starts to decrease, which is accompanied by an increase of the phase factor. Such a change of phase indicates that above 1.7 kV, the leakage current increases, and the character of the specimen changes from dielectric to more resistive. The voltage withstanding condition may be attributed simply to a voltage range, where the impedance characteristic remains insignificantly affected by the applied voltage i.e., the specimen current is a linear function of the specimen voltage.

Fig. 4 shows voltage waveforms that are representative for the high-k composite films. A distortion in the response waveform $v_R(t)$ indicates nonlinear dielectric effects. The
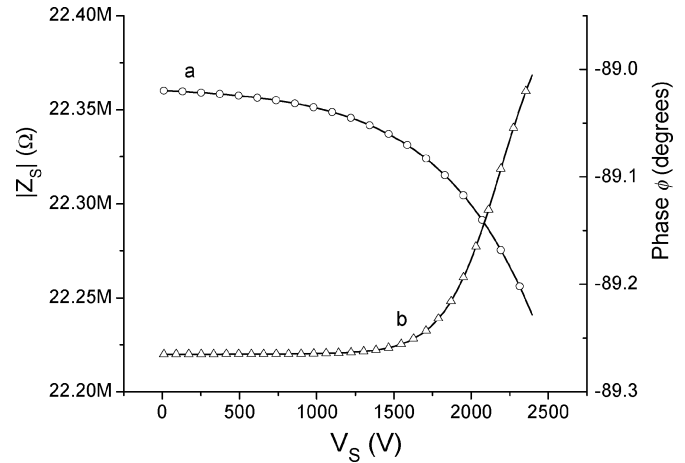

Fig. 3.   (a) Impedance magnitude and (b) phase angle for FR-4 specimens.
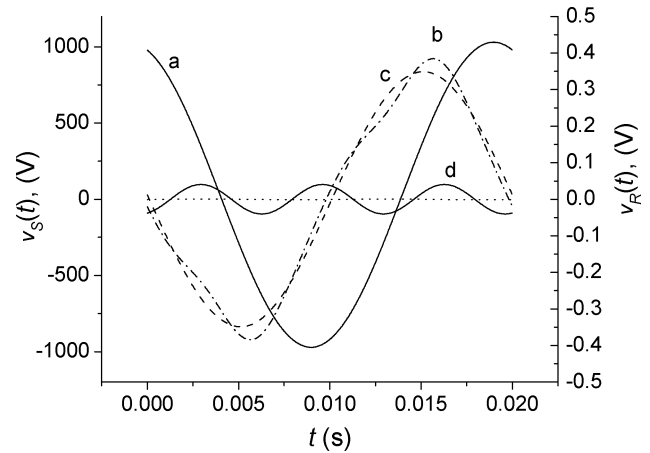

Fig. 4.   Voltage waveforms for high-dielectric constant composites ($k = 12$): (a) $-v_S(t)$, (b) $-v_R(t)$, (c) first fundamental, and (d) third harmonic. The amplitude of the second harmonic is much smaller than the amplitude of the third harmonic and cannot be seen in the plot.

$v_R(t)$ waveform can be represented as a superposition of the fundamental [Fig. 4(c)] and higher order harmonics, where the third-order harmonic wave [Fig. 4(d)] is the main nonlinear component in the total response. In comparison to FR-4, the impedance of the high-k specimens decreases considerably with increasing voltage, which leads to an increased specimen current. The impedance and phase plots obtained for high–k materials as a function of the specimen voltage are shown in Fig. 5. The drop in impedance is accompanied by a significant change in phase. Under the applied electric field, the material undergoes an apparent transformation from dielectric to resistive. A comparison of the specimen-equivalent impedance indicates that the linear voltage range is much narrower for the high-k organic composites than that for the conventional dielectrics, suggesting that these materials would withstand only a small fraction of the conventionally measured dielectric withstanding voltage. At a sufficiently high power level, such behavior may lead to thermal run-away due to an excess of dissipated current. This mechanism is fundamentally different than the dielectric breakdown that occurs in typical dielectric materials, where the dielectric failure is due primarily to voltage excited avalanche ionization.
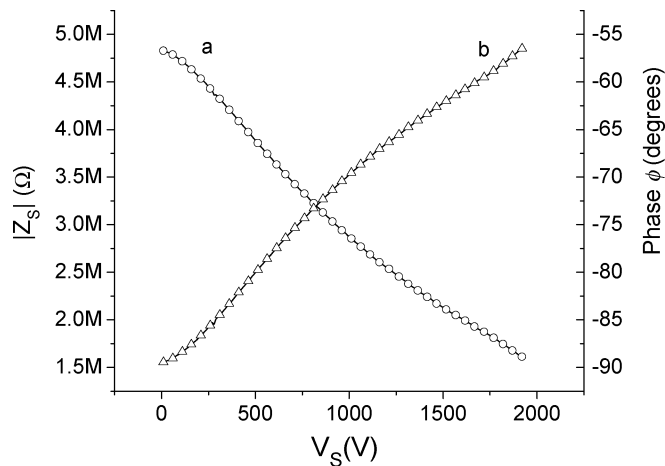
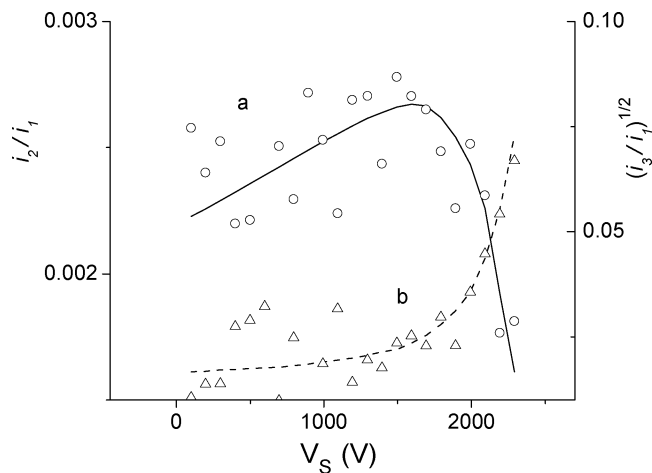Fig. 5. (a) Impedance magnitude and (b) phase angle of high-dielectric constant composites ($k = 12$).

Fig. 6. Normalized amplitude of the (a) second-harmonic and (b) third-harmonic current response for the FR-4 material as a function of the specimen voltage.
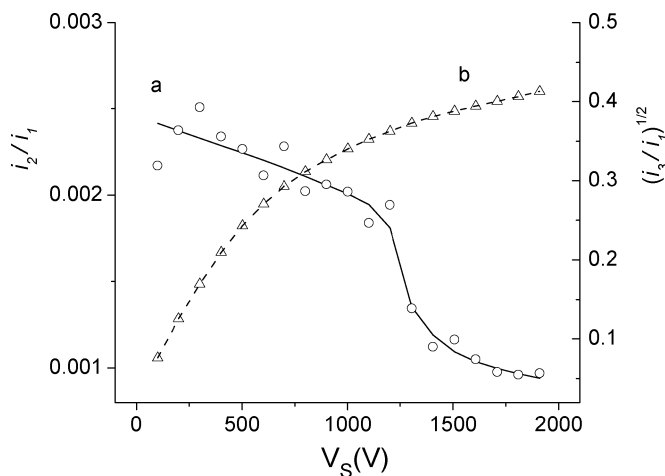

Fig. 7. Normalized amplitude of the (a) second-harmonic and (b) third-harmonic current response for the high-dielectric constant composite as a function of the specimen voltage.

To analyze the nonlinear dielectric effects in more detail, we calculated the relative amplitude of the higher order harmonic currents (i_n/i_1), using (10). Figs. 6 and 7 illustrate these results for both types of materials, where the relative amplitude of the second harmonic (i_2/i_1) and the square root of the third

harmonic $(i_3/i_1)^{1/2}$ are plotted as a function of the specimen voltage. Since the fundamental i_1 is linearly dependent on voltage, the slope of the (i_2/i_1) plot is proportional to the relative magnitude of the second-order dielectric susceptibility, while the slope of the $(i_3/i_1)^{1/2}$ plot reflects the relative magnitude of the third-order susceptibility [6]. In the case of FR-4 specimens, the normalized second-harmonic current (i_2/i_1) increases linearly with the specimen voltage, reaching a maximum at about 1.6 kV [Fig. 6(a)]. This second-order nonlinear dielectric susceptibility, which originates from a residual static polarization, disappears above 1.7 kV. Thus, the voltage range where (i_2/i_1) decreases can be attributed to a voltage-driven molecular rearrangement process where the material approaches near-dielectric-breakdown conditions. In comparison, the $(i_3/i_1)^{1/2}$ plot [Fig. 6(b)] changes slope at about 1.7 kV, again indicating a voltage-induced molecular mobility, which results in an increased third-order dielectric susceptibility above 1.7 kV. Fig. 7 shows the corresponding amplitude of the second-harmonic and the third-harmonic currents obtained for the high-k dielectric material. As shown, the third-order susceptibility dominates the overall nonlinear dielectric response at all voltages. Such behavior can be attributed to the polarization reversal in a ferroelectric ceramics component dispersed in the organic phase. Polarization reversal in ferroelectric materials usually generates odd-order harmonics, where the magnitude of the third harmonic is typically the largest. The change in slope of the $(i_3/i_1)^{1/2}$ plot [Fig. 7(b)] at about 700 V indicates a change in the dielectric polarization mechanism of the ceramic filler rather than a dielectric softening of the organic phase. Initially large, the third-order susceptibility tensor decreases above 700 V, due to ferroelectric saturation in the ceramic filler. Consequently, the overall character of the third-harmonic response is fundamentally different than that shown in Fig. 6(b) for FR-4 specimens. Both the impedance characteristic [Fig. 5] and the third-order nonlinear dielectric response [Fig. 7(b)] reflect primarily the dielectric properties of the ceramics rather than organic phase. However, in the background of the third-harmonic response, the second harmonic is present [Fig. 7(a)]. The normalized second-harmonic current (i_2/i_1) decreases somewhat with the increasing specimen voltage up to about 1.2 kV. The (i_n/i_1) drops rapidly above 1.2 kV, which can be interpreted as near-dielectric-breakdown conditions. Therefore, the dielectric-breakdown conditions are initiated at about 1.2 kV for this material.

It should be noted that the presented procedure of recording and analyzing waveforms allows the evaluation of specific characteristics of materials that cannot be readily evaluated using conventional techniques. This measurement procedure is especially suitable for detecting and analyzing nonlinear dielectric effects that can result from polarization reversal, rectifying barriers, and material degradation near-dielectric-breakdown conditions. Such effects may appear at relatively low voltages in nano-sized interfaces, composites, and submicrometer thin dielectric films that are of interest to new technologies. The presented results demonstrate that the dielectric-breakdown conditions can be inferred from the impedance characteristic and nonlinear dielectric response without ambiguity. In industrial practice, ac high voltage testing is performed at either 50 or

60 Hz. Certain applications, such as switching power suppliers, may require testing at higher frequencies. At higher frequencies, the impedance of capacitive specimens with a complex capacitance C^* will decrease ($Zc = 1/2\pi f C^*$), which will lead to a larger current drained from the power source. In addition, higher order susceptibilities may reflect the frequency-dependent properties of materials. The implemented instrumentation is capable of operating at frequencies of up to about 100 kHz. In general, the presented theoretical analysis is based on the assumption of quasi-static conditions, where the circuit consists only of lumped elements. Therefore, (9) is not valid at higher frequencies where the propagation effects may not be neglected, i.e., the length of the propagating wave is comparable with the size of the circuit elements.

V. CONCLUSION

We demonstrated a waveform technique to measure complex impedance of dielectric films at high ac voltages by recording and analyzing the incident voltage and the resulting dissipation current waveforms using multichannel data acquisition (DAQ) instrumentation. This procedure is capable of resolving the phase component between the specimen voltage and the specimen current and is thus suitable for determining the specimen complex impedance. It can also be utilized to analyze the nonlinear dielectric response of materials and to determine the mechanism of their dielectric breakdown. Conventional dielectrics, such as FR-4, exhibit a flat impedance characteristic nearly independent of voltage up to the materials' breakdown conditions. In contrast, the impedance of dielectric hybrid materials made of organic resins and high-dielectric constant ceramics decreases considerably with increasing voltage, making it difficult to determine the dielectric withstanding voltage. The results demonstrate, however, that the voltage withstanding condition can be inferred from the second-order and third-order susceptibility characteristics. The presented testing procedure represents a compatible extension of the existing standard test methods for evaluating dielectric breakdown but is better suited for low-impedance thin-film materials and materials with a high-dielectric constant.

REFERENCES

[1] *Dielectric Breakdown Voltage of Solid Electrical Insulating Materials at Commercial Power Frequencies*, ASTM D149-97a, 1997.

[2] R. Reid, "High voltage VLF test equipment with sinusoidal waveform," in *Proc. IEEE Transmission Distribution Conf.*, vol. 1, Apr. 11–16, 1999, pp. 8–12.

[3] S. K. Venkatesh and M. S. Naidu, "A test setup with automated measurements for impulse voltage breakdown studies of gaseous insulation," in *Proc. IEEE 11th Int. Symp. High Voltage Engineering*, vol. 1, Aug. 23–27, 1999, Conf. Publ. no. 467, pp. 181–184.

[4] A. Tanaka, K. Tohyama, T. Tokoro, M. Kosaki, and M. Nagao, "High field dissipation current waveform of polyethylene film obtained by new method," in *IEEE Annu. Rep. Conf. Electrical Insulation Dielectric Phenomena*, Oct. 20–24, 2002, pp. 610–613.

[5] A. Tanaka, K. Tohyama, M. Nagao, T. Tokoro, and M. Kosaki, "Improvements of high accuracy AC dissipation current waveform observation system," in *Proc. Int. Symp. Electrical Insulating Materials (ISEIM 2001)*, Nov. 19–22, 2001, pp. 423–426.

[6] T. Furukawa, K. Nakajima, T. Koizumi, and M. Date, "Measurement of nonlinear dielectricity in ferroelectric polymers," *Jpn. J. Appl. Phys.*, vol. 26, pp. 1039–1045, 1987.

[7] *IEEE Standard for Terminology and Test Methods for Analog-to-Digital Converters*, IEEE Standard 1241-2000, 2000.

[8] *Theory of Discrete and Continuous Fourier Analysis*, H. J. Weaver, Ed., Wiley, New York, 1989, p. 237.

[9] K. Hejn and S. Pacut, "Effective resolution of analog to digital converters," *IEEE Instrum. Meas. Mag.*, vol. 6, no. 3, pp. 48–55, Sep. 2003.

Jan Obrzut (M'00) received the Ph.D. degree in technical sciences from the Institute of Physics, Cracov Polytechnic, Poland, in 1981.

After a postdoctoral appointment at the Polymer Science Department, University of Massachusetts, Amherst, he was a Researcher at the Five College Radio Astronomy Department, University of Massachusetts, working on microwave dielectric waveguides. In 1988, he joined IBM as Advisory Engineer, where he conducted exploratory work on the application of polymer dielectrics in microelectronics. Since 1997, he has been with the Polymers Division of the National Institute of Standards and Technology (NIST), Gathersburg, MD, where he pursues research in metrology of dielectric films and hybrid materials for microwave and electronic applications. His research interests include embedded passive devices and organic electronic materials.

Kenji Kano received the Ph.D. degree in polymer chemistry from the Department of Chemistry, Faculty of Science, Tokyo University of Science, Tokyo, Japan, in 2002.

Since 2002, he has been a Guest Researcher at the Polymers Division, National Institute of Standards and Technology (NIST), Gaithersburg, MD. His current research interests include ion-conducting mechanisms in polymers, the ferroelectric switching process, broadband permittivity, and electrical properties of organic electronic materials.